Proc. Natl. Acad. Sci. USA
Vol. 95, pp. 13652–13657, November 1998
Cell Biology

Myosin II localization during cytokinesis occurs by a mechanism that does not require its motor domain

JI-HONG ZANG AND JAMES A. SPUDICH*

Department of Biochemistry, Stanford University, Stanford, CA 94305

Contributed by James A. Spudich, September 15, 1998

ABSTRACT **Myosin II generates force for the division of eukaryotic cells. The molecular basis of the spatial and temporal localization of myosin II to the cleavage furrow is unknown, although models often imply that interaction between myosin II and actin filaments is essential. We examined the localization of a chimeric protein that consists of the green fluorescent protein fused to the N terminus of truncated myosin II heavy chain in *Dictyostelium* cells. This chimera is missing the myosin II motor domain, and it does not bind actin filaments. Surprisingly, it still localizes to the cleavage furrow region during cytokinesis. These results indicate that myosin II localization during cytokinesis occurs through a mechanism that does not require it to be the force-generating element or to interact with actin filaments directly.**

Conventional myosin II is a hexameric molecule composed of two heavy chains, two essential light chains (ELCs), and two regulatory light chains (RLCs). Each heavy chain consists of a globular catalytic domain, an ELC-binding site, an RLC-binding site, and an α-helical coiled-coil rod (Fig. 1 *Upper*). Myosin II is a major component of the cellular machinery responsible for cell division (1, 2). However, little is known about how myosin localizes into the cleavage furrow region during cytokinesis. We use the cellular slime mold *Dictyostelium discoideum* as a model system to study myosin localization. *Dictyostelium* cells lacking functional myosin II are unable to undergo cytokinesis in the absence of adhesion (3–5). On an adhesive surface, however, these cells can undergo cell cycle-controlled, mitosis-coupled divisions (5, 6). In these myosin II-null cells, we expressed a chimeric protein, GFP-RLC-myosin rod, in which the GFP is attached to the N terminus of a truncated myosin II heavy chain, composed of the RLC-binding site and the α-helical coiled-coil rod (Fig. 1 *Lower*). Lacking the first 787 amino acids of myosin II heavy chain, the chimera is missing most of the globular subfragment-1 domain, which is known to bind and move actin filaments (7–9). Studying the localization of this chimera enables us to test models of myosin II localization that require myosin II to interact directly with actin filaments, and thus gives us insights into the molecular mechanism of myosin II localization.

MATERIALS AND METHODS

Plasmid Construction. The plasmids were constructed to fuse the gene for GFP to the DNA encoding the RLC-binding region of the heavy chain. Three additional amino acids, Ala-Ala-Gly, link GFP to the truncated myosin II heavy chain. The N terminus of the light chain binding region of the myosin II heavy chain was obtained by carrying out the polymerase chain reaction (PCR) with the primer 5′-CGCGCTGCAG-GTCACACTGTTGCTGCTCG-3′, which added a *Pst*I site, and another primer corresponding to sequences inside the myosin II gene (5′-TCTAAGGCATCCTTGCTAT-3′). The template used was pMyDap. The resulting 320-bp product was digested with *Pst*I and *Nco*I and ligated to pMyDap, which was similarly digested with *Pst*I and *Nco*I. This plasmid was named pRLC+. The gene for GFP with *Pst*I restriction sites was obtained by using PCR. The primers were designed to introduce the linkers, as well as sites for the enzyme *Pst*I. The gene for GFP was obtained by using PCR with an M13 forward primer (5′-GTCACGACGTTGTAAAACGACGGC-CAGTG-3′) and Pst-GFP-end2 (5′-CGCGCTGCAGCTTT-GTATAGTTCATCCATGCCATG-3′). The template used was pTZ18R-GFPN, which contains a *Pst*I site upstream of the *Dictyostelium* actin 15 promoter fused to the GFP gene. Next the GFP PCR product was digested with *Pst*I and inserted into pRLC+. The plasmid with the correct orientation was selected. Then the desired GFP-RLC+ was digested with *Xba*I and *Sac*I and put into an expression vector, pBIG, similarly digested, resulting in pBIG-GFP-RLC+. The sequences were confirmed by DyeDeoxy terminator cycle sequencing reactions (Applied Biosystems).

Cell Culture. HS1, a myosin II-null cell line (10), was transformed with pBIG-GFP-RLC+. Individual clones were grown at 21°C in HL5 medium (11), supplemented with Pen-Strep (60 units/ml penicillin; 60 μg/ml streptomycin), and 5 μg/ml of G418 (Geneticin; Life Technologies, Gaithersburg, MD).

Protein Purification. Myosin II and GFP-RLC-myosin rod were purified according to Ruppel *et al.* (10) with modifications. Cells were lysed in 25 mM Hepes, pH 7.4/50 mM NaCl/2 mM EDTA/1 mM DTT buffer with 0.5% Triton X-100. The pellet was washed in the same buffer without Triton and resuspended in a buffer of 10 mM Hepes, pH 7.4/300 mM NaCl/3 mM $MgCl_2$/2 mM ATP/1 mM DTT. The supernatant was dialyzed against 10 mM Pipes, pH 6.8/50 mM NaCl/10 mM $MgCl_2$/1 mM DTT for the reformation of the higher-order assemblies. A second assembly/disassembly cycle followed. The pellet from the dialysis was then resuspended in a buffer of 10 mM Hepes, pH 7.4/300 mM NaCl/3 mM $MgCl_2$/2 mM ATP/1 mM DTT. The supernatant was again dialyzed into Pipes buffer, pH 6.8/50 mM NaCl. The pellet was collected from that solution and resuspended in 10 mM Hepes, pH 7.4/200 mM NaCl/1 mM $MgCl_2$/0.5 mM ATP/1 mM DTT. Protein concentration was determined by using the Bradford assay (12), with rabbit skeletal myosin as the standard. The yield varies from preparation to preparation, but is typically 2–3 mg of protein from 15 g of wet cells.

Immunoblots. Equal volumes of *Dictyostelium* whole cell lysates, at 10^7 cells per ml, were loaded onto two SDS/7.5% polyacrylamide gels. These gels were then either stained with Coomassie brilliant blue or transferred onto nitrocellulose paper. The blot was probed with My6, an anti-*Dictyostelium*

The publication costs of this article were defrayed in part by page charge payment. This article must therefore be hereby marked "*advertisement*" in accordance with 18 U.S.C. §1734 solely to indicate this fact.

Abbreviations: GFP, green fluorescent protein; ELC, essential light chain; RLC, regulatory light chain.

*To whom reprint requests should be addressed at: Department of Biochemistry, Beckman Center B400, Stanford University, Stanford, CA 94305. e-mail: jspudich@cmgm.stanford.edu.

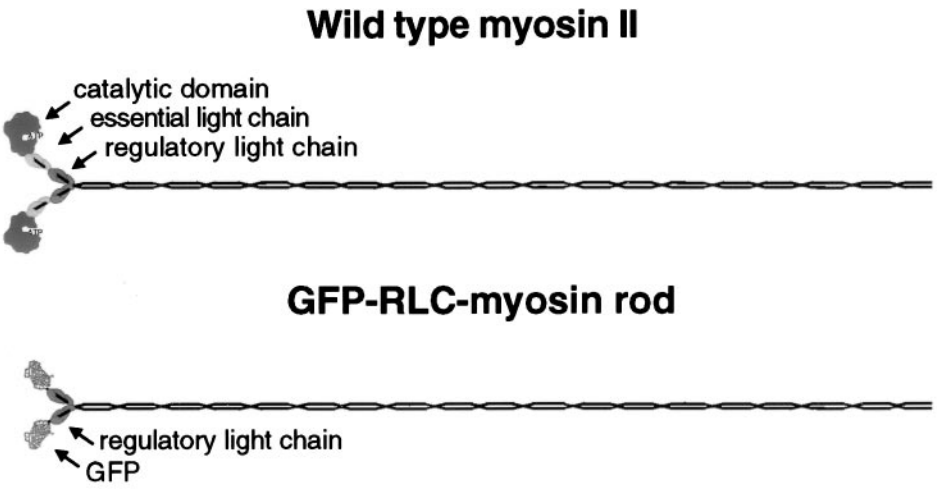

FIG. 1. Schematic drawings of wild-type myosin II and green fluorescent protein (GFP)-RLC-myosin rod. Wild-type myosin II is a hexameric molecule composed of two heavy chains, two ELCs, and two RLCs. Each heavy chain consists of a catalytic domain, which binds and moves actin filaments, an ELC-binding site, an RLC-binding site, and a rod. In the chimeric protein GFP-RLC-myosin rod, GFP is fused to a truncated myosin II heavy chain that is missing the catalytic domain and the ELC-binding site.

myosin II monoclonal antibody (13), followed by a goat anti-mouse secondary antibody conjugated to horseradish peroxidase (Bio-Rad). An enhanced chemiluminescence system (Amersham) was used to visualize the signals. To visualize the light chains and the heavy chain, 3 μg of purified protein per lane was loaded onto two SDS/15% polyacrylamide gels. One gel was stained with Coomassie brilliant blue. The protein on the other gel was transferred onto nitrocellulose and probed with My8 (13), a monoclonal anti-RLC antibody, to visualize the light chain.

Cosedimentation. Purified wild-type myosin or GFP-RLC-myosin rod at 0.1 mg/ml in a buffer of 10 mM Hepes, pH 7.4/250 mM NaCl/1 mM DTT/5 mM EDTA was incubated on ice for 15 min with or without 0.2 mg/ml rabbit muscle actin. Then they were centrifuged in a TL100.1 rotor (Beckman) at 4°C for 10 min at 75,000 rpm. The supernatant and the pellet portions were loaded onto an SDS/12.5% polyacrylamide gel, followed by staining with Coomassie brilliant blue.

Electron Microscopy. Purified GFP-RLC-myosin rod at 2 mg/ml in 10 mM Hepes buffer (pH 7.4) with 300 mM NaCl, 1 mM DTT, and 3 mM $MgCl_2$, was rapidly diluted 1:10 into 10 mM Hepes buffer (pH 7.4) with 50 mM NaCl, 1 mM DTT, and 10 mM $MgCl_2$ and deposited onto Formvar-covered copper grids. A 1% uranyl acetate solution was used to negatively stain the protein sample. Specimens were examined with a Philips 410 electron microscope.

Salt Dependence Filament Assay. This assay was done as described by Moores *et al.* (14). Proteins at 0.2 mg/ml in different buffers with various salt concentrations were centrifuged at 55,000 rpm, 4°C, for 10 min in a TL100.1 rotor. The supernatant fractions containing monomeric proteins were analyzed with the Bradford assay (12). The fraction soluble was calculated by dividing the amount of protein in the supernatant by the total protein.

Fluorescence Microscopy. Cells were placed in Mes buffer [20 mM 2-(morpholino)ethanesulfonic acid, pH 6.8/0.2 mM $CaCl_2$/2 mM $MgSO_4$] at 22°C. Imaging was done as previously described (15).

RESULTS AND DISCUSSION

We have constructed a chimeric protein, GFP-RLC-myosin rod, in which GFP is attached to the N terminus of a truncated *Dictyostelium* myosin II heavy chain, consisting of the RLC-binding domain and the α-helical region that forms the myosin II rod (Fig. 1).

We isolated independent clones expressing GFP-RLC-myosin rod in *Dictyostelium* cells lacking their single endogenous myosin II heavy chain gene (10). The expression level of GFP-RLC-myosin rod is comparable to that of myosin II in wild-type cells (Fig. 2). GFP-RLC-myosin rod migrates faster than wild-type myosin II in SDS/PAGE, consistent with it being about 60 kDa smaller than wild-type myosin II. It also appears as a single band in the clone we isolated, demonstrating that these cells are expressing only the chimeric protein, and not both the chimera and the wild-type myosin II. Like myosin II-null cells, cells expressing the chimera do not grow in suspension or complete developmental changes critical for spore formation (3, 4) (data not shown).

We then investigated whether a lack of motor domain affected the ability of the chimeric protein to form bipolar

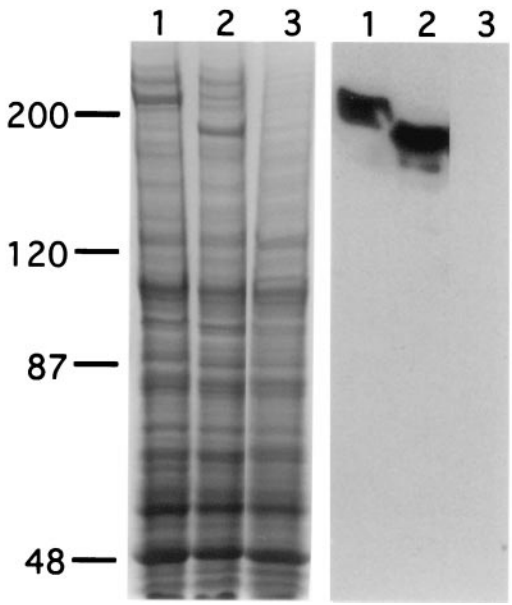

FIG. 2. GFP-RLC-myosin rod is expressed at levels similar to those of wild-type myosin II in *Dictyostelium* cells. Whole cell lysates of cells expressing wild-type myosin II (lane 1), GFP-RLC-myosin rod (lane 2), or no myosin II (lane 3) were analyzed on an SDS/7.5% polyacrylamide gel. (*Left*) Coomassie brilliant blue staining. (*Right*) An immunoblot of the whole cell lysates using an anti-myosin II antibody demonstrates that the appropriate proteins are expressed in comparable amounts.

thick filaments. Monomeric myosin II molecules assemble to form bipolar thick filaments, which are the functional forms of myosin II *in vivo* (16). In low-salt buffers with 10 mM $MgCl_2$, purified wild-type myosin II molecules form bipolar thick filaments 0.6–0.8 μm in length, with 0.13–0.19 μm long bare zones (17). As examined by electron microscopy, GFP-RLC-myosin rod also forms individual thick filaments that are clearly bipolar in a buffer containing 50 mM NaCl and 10 mM $MgCl_2$ (Fig. 3*A*). Furthermore, the average length of bipolar thick filaments formed by the chimeric protein is 0.45 μm long (standard deviation = 0.06, n = 113), and the average bare zone length is 0.19 μm (standard deviation = 0.03, n = 63). These measurements are similar to those of the wild-type myosin. In the absence of $MgCl_2$, the chimeric protein forms looser filamentous structures (data not shown), similar to those seen with wild-type myosin II in the absence of $MgCl_2$ (17).

Filament formation *in vitro* depends on the salt concentration. GFP-RLC-myosin rod is mostly monomeric in buffer with 0 mM salt, assembles in 50 mM NaCl, and then returns to the monomeric state in high salt (Fig. 3*B*). The salt-dependent assembly properties of the chimeric protein are very similar to those of the wild-type myosin II assayed under the same conditions (14).

We also assayed for GFP-RLC-myosin rod's ability to bind RLC, since it has an RLC-binding site. Fig. 4*A* shows proteins enriched from *Dictyostelium* whole cell lysates after two rounds of filament assembly and disassembly in buffers with appropriate salt concentrations. The second pellets are shown. The RLC, but not the ELC, is bound to the chimera as predicted (Fig. 4*A*, GR), whereas both light chains bind to the wild-type myosin II (Fig. 4*A*, WT). Immunoblots probed with anti-RLC antibody confirmed that the 18-kDa protein is RLC.

Because the actin-binding site of myosin II is on the catalytic domain (7), which is missing in the chimera, GFP-RLC-myosin rod molecules do not bind to actin. Note that the wild-type myosin II preparation retains a significant amount of actin at this point in the purification, whereas the GFP-RLC-myosin rod preparation does not. To confirm that GFP-RLC-myosin rod does not interact with actin, we performed a cosedimentation assay (Fig. 4*B*). Purified wild-type myosin or GFP-RLC-myosin rod was incubated with or without actin filaments in a buffer with 250 mM NaCl. At this salt concentration, most of the myosin II or GFP-RLC-myosin rod molecules are monomeric and thus stay in the supernatant. A small portion of protein forms higher-order structures and sediments into the pellet. When actin filaments were added, however, all of the wild-type myosin went into the pellet, whereas no additional GFP-RLC-myosin rod sedimented in the presence of actin compared with sedimentation in its absence. Therefore, unlike wild-type myosin II, the chimera cannot interact directly with actin filaments.

The biochemical assays indicate that the chimeric protein, GFP-RLC-myosin rod, behaves as we would expect a myosin II without its catalytic domain and its ELC-binding domain. The enzymatic properties, such as actin binding, are generally attributed to the globular catalytic domain (7–9), whereas filament formation depends on a functional α-helical myosin rod (18). Indeed, not only does GFP-RLC-myosin rod form bipolar thick filaments in sizes similar to wild-type myosin II (Fig. 3*A*) but also its salt-dependent filament formation parallels myosin II (Fig. 3*B*). Furthermore, the chimera binds RLC, but unlike wild-type myosin II, it does not bind ELC (Fig. 4*A*). Most importantly, it does not interact with actin filaments, as shown by the cosedimentation assay (Fig. 4*B*). Moreover, *in vivo*, it is expressed at a level that is similar to myosin II in wild-type cells. With such a tool in hand, we proceeded to examine the localization of this chimeric protein in live cells by using fluorescence microscopy.

Although *Dictyostelium* cells lacking functional myosin II are unable to divide in suspension, they can still divide on an adhesive surface by a cell cycle-regulated, mitosis-coupled process, which we term cytokinesis B (5). We examined the localization of GFP-RLC-myosin rod in cells during cytokinesis B by fluorescence microscopy. Examples of typical GFP-RLC-myosin rod cells undergoing division on a surface are shown in Fig. 5 *C* and *D*. During cytokinesis, the *Dictyostelium* cell nucleus did not break down (19), and the nuclei appeared as areas of reduced fluorescence because GFP-RLC-myosin rod was excluded. Cells first rounded up during early mitosis. At this stage, GFP-RLC-myosin rod was diffusely distributed throughout the cell (Fig. 5 *C* and *D*, time 0:00).

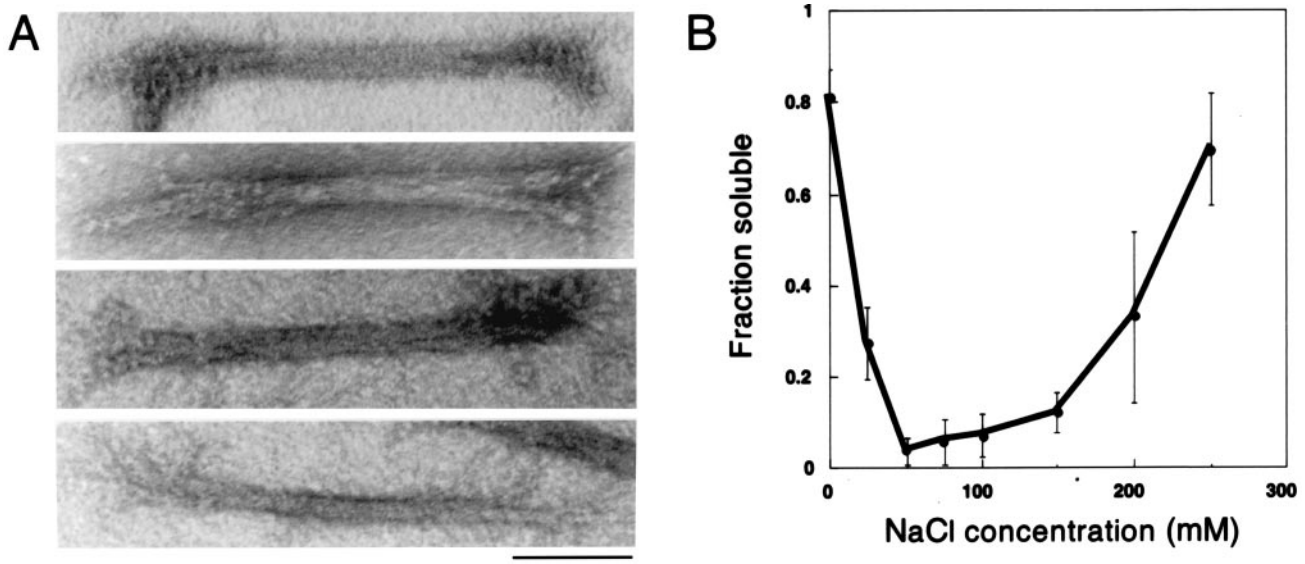

FIG. 3. GFP-RLC-myosin rod has filament formation characteristics similar to those of wild-type myosin II. (*A*) Negatively stained bipolar thick filaments of GFP-RLC-myosin rod formed in a buffer containing 50 mM NaCl and 10 mM $MgCl_2$. (Bar, 0.1 μm.) (*B*) Purified proteins were dissolved in buffer containing NaCl at various concentrations. Centrifugation separated the solubilized protein, which remained in the supernatant, from the higher-order assemblies in the pellet. GFP-RLC-myosin rod has salt-dependent assembly characteristics similar to those of wild-type myosin II assayed under the same conditions. The mean fraction soluble is plotted for each salt concentration, and the error bars represent the standard deviation from seven experiments.

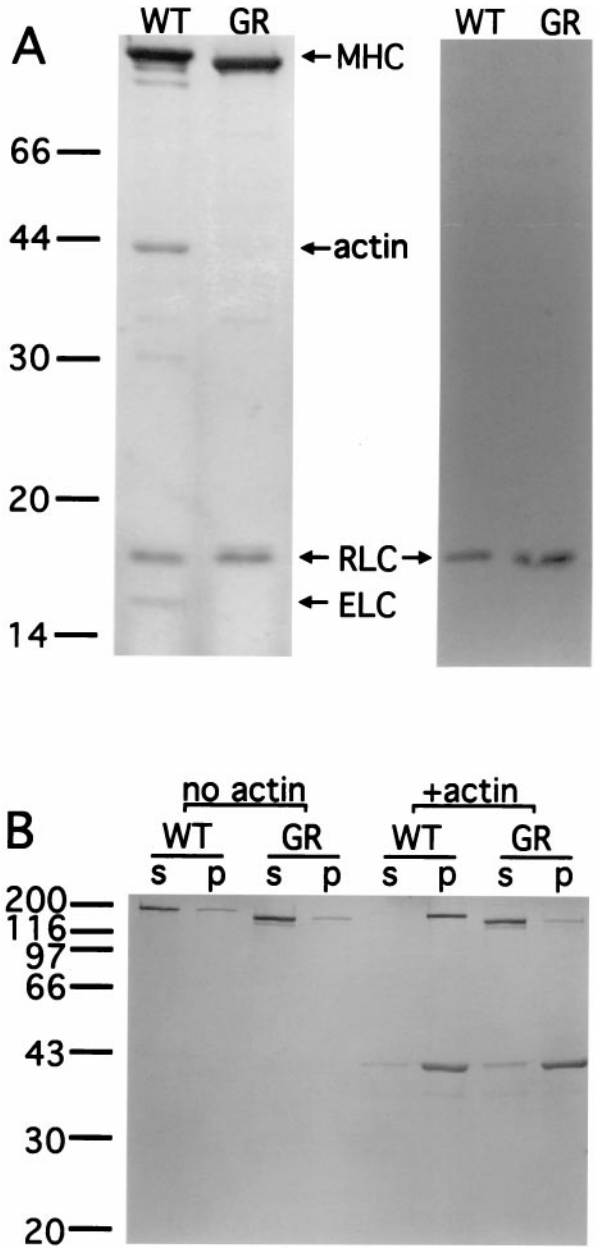

FIG. 4. GFP-RLC-myosin rod binds RLC but does not interact with actin. (*A*) (*Left*) Wild-type myosin II and GFP-RLC-myosin rod were partially purified from whole cell lysates by two rounds of assembly and disassembly, and the second pellets are shown. Wild-type myosin II (WT) purifies with both light chains bound, whereas the GFP-RLC-myosin rod (GR) purifies only with RLC, as expected. Note that the wild-type myosin II copurifies with a significant amount of actin, which is not the case for the GFP-RLC-myosin rod because it lacks the actin-binding domain. (*Right*) Western blot probed with anti-RLC antibody confirms the identity of the RLC. (*B*) Purified wild-type myosin or GFP-RLC-myosin rod at 0.1 mg/ml in a buffer of 10 mM Hepes, pH 7.4/250 mM NaCl/1 mM DTT/5 mM EDTA were incubated for 15 min with or without actin on ice and then centrifuged at 55,000 rpm in a TL100.1 rotor at 4°C. In the absence of actin, most wild-type myosin II or GFP-RLC-myosin rod remained in the supernatant. With the addition of 0.2 mg/ml actin, all wild-type myosin II molecules sedimented into the pellet along with actin filaments. However, GFP-RLC-myosin rod molecules were not affected by the sedimentation of actin filaments; most remained in the supernatant. s, Supernatant; p, pellet.

After the nuclear division, diffuse small aggregates started to appear and to concentrate between the nuclei. As the cell stretched out, the aggregates became more concentrated in the furrow region. Such behavior was observed in all 21 cells examined. Finally, the daughter cells separated and migrated with GFP-RLC-myosin rod concentrated in their posterior region. Eight of the 21 cells had symmetrical GFP-RLC-myosin rod distributions in daughter cells of similar sizes, as exemplified by the cells in Fig. 5 *C* and *D*. Eleven of the 21 cells distributed myosin II asymmetrically to the posterior regions of the daughter cells. Eight of these 11 had daughter cells of different sizes, with most of the GFP-RLC-myosin rod going to the larger daughter cell (data not shown). Asymmetrical distribution of myosin II is also seen in GFP-myosin II cells, although much less frequently. Daughter cells of significantly different sizes are not seen in GFP-myosin II cells (J. Sabry, S. Ryan, and J.A.S., unpublished observations), but are common in surface-dependent divisions with myosin II-null cells (5). In two cases, GFP-RLC-myosin rod cells failed to divide (data not shown). We also observed three division events of binucleate cells, in which GFP-RLC-myosin rod was concentrated in the middle of the four separating daughter cells (data not shown). The concentration of GFP-RLC-myosin rod is not an artifact, since cells expressing GFP alone (20), or GFP-3xASP-myosin II (15) (Fig. 5*B*), a mutant myosin II which cannot assemble into bipolar thick filaments, did not concentrate in the furrow region during cytokinesis B. Importantly, while the localization of GFP-RLC-myosin rod is in the furrow region, it is different from GFP-myosin II localization in *Dictyostelium* cells in that the localization of the chimera is not cortical (15) (compare Fig. 5*A* with 5 *C* and *D*).

How does myosin II localize to the cleavage furrow during cytokinesis? One favorite hypothesis has been that myosin II localizes by cortical flow, driven by a gradient of tension that pulls the cortical elements from regions of relaxation (the poles) to regions of tension (the furrow) (21). During cytokinesis, the gradient could be set up by equatorial stimulation (22) or polar relaxation (23). In the equatorial stimulation model, a small amount of myosin II could be stimulated to move into the furrow region, setting up a gradient, causing the rest of the myosin II in the cortex to follow (22). In the polar relaxation model, myosin II localizes to the cleavage furrow because of a gradient of cortical tension generated by myosin II motor activity after relaxation of the polar cortex. Regardless of the region of initial stimulation, myosin II could generate the force necessary for the tension gradient. Recently, Yumura and Uyeda showed that a *Dictyostelium* myosin II mutant that can bind actin filaments but has markedly reduced motor activity can still localize to the cleavage furrow in *Dictyostelium* cells at the same rate as wild-type myosin II (24). They hypothesized that these mutants are passively transported into the cleavage furrow through direct association with actin, and that cortical flow is powered by other motor proteins. Our finding that a chimeric protein without any myosin II motor activity or actin-binding site can still localize to the cleavage furrow provides strong evidence that none of these proposed mechanisms are required for myosin II localization during cytokinesis.

A very important aspect of the localization of the GFP-RLC-myosin rod to the furrow region is that, unlike GFP-myosin II, the GFP-RLC-myosin rod is cytoplasmic rather than cortical. Our current working hypothesis for assembly of the myosin II-containing contractile ring, therefore, is one in which the myosin II is brought to the furrow region through the cytoplasm, independent of the cortical actin assembly, and is then pulled into the cortex in that region by way of functional interaction with the cortical actin. Once the actin-myosin II complex is formed in the cortical portion of the furrow region, force can be produced for the constriction of the furrow. While the molecular basis of the establishment of myosin II in the furrow region is not understood, it is clear from these studies that it is independent of the actin-binding motor domain of the myosin II molecule. Myosin II could be somehow guided to the

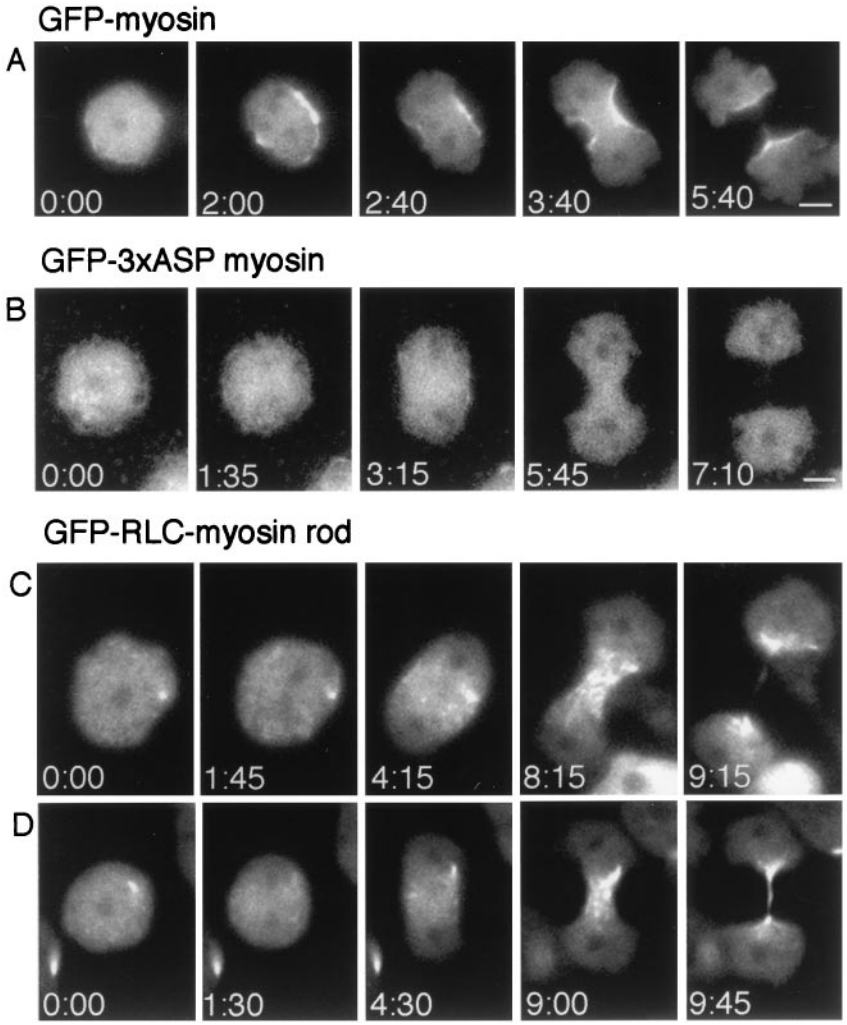

FIG. 5. Myosin II-null cells expressing various GFP proteins undergoing division on a surface. GFP-myosin II and GFP-RLC-myosin rod, but not GFP-3xASP myosin II, are localized to the cleavage furrows. (*A* and *B*) Time-lapse fluorescence microscopy captures division of a cell expressing GFP-myosin II, which is localized to the cortex of the cleavage furrow (*A*), and division of a cell expressing GFP-3xASP-myosin II, which is diffuse throughout the cell during the adhesion-dependent, myosin II-independent cytokinesis B process (*B*) (5). (Bars, 5 μm.) (*C* and *D*) Symmetrical divisions by the myosin II-independent cytokinesis B process in which the GFP-RLC-myosin rod is distributed equally to daughter cells of similar sizes. GFP-RLC-myosin rod is localized to the cleavage furrow region, but differs from GFP-myosin II in that GFP-RLC-myosin rod is not cortical.

furrow by accessory proteins that recognize the myosin II tail, and such proteins are worth searching for. Intriguingly, myosin II does not localize to the furrow region in clathrin heavy chain-null mutants of *Dictyostelium* (25). This observation might imply that myosin II transporters could be membranous elements, perhaps driven along microtubules by kinesin-like motors, as suggested by Vallee *et al.* (26). Kinesin-dependent movement of myosin II could also be independent of membranes. Interestingly, *Drosophila* cells expressing mutated KLP3A, a kinesin-like protein, fail to form a contractile ring during meiosis, whereas anaphase is not affected (27). Actin is not localized to the cleavage furrow region in these cells (28). Similarly, *Drosophila* cells with mutations in *pavarotti*, which encodes a kinesin-like protein related to the mammalian MKLP-1, undergoes normal anaphase but forms abnormal telophase spindle and fails in cytokinesis in mitotic cycle 16 (29). Again, contractile ring proteins, such as actin and anillin, were not localized in the furrow region in these mutant cells (29). While highly speculative, this concept of kinesin-dependent myosin II localization might explain the well known connection between microtubule and contractile ring localization (30, 31).

We thank Sheri Moores for imaging the GFP-3xASP myosin II cell, Shannon Ryan for imaging the GFP-myosin II cell, Amit Mehta for providing the purified wild-type myosin II protein for the cosedimentation assay, and Fran Thomas for her help with electron microscopy. We also thank Hans Warrick, Doug Robinson, and Coleen Murphy for comments on the manuscript. This work was supported by a grant from the National Institutes of Health (GM40509) to J.A.S., and J.Z. is supported by a predoctoral fellowship from the Howard Hughes Medical Institute.

1. Mabuchi, I. & Okuno, M. (1977) *J. Cell Biol.* **74,** 251–263.
2. Satterwhite, L. L. & Pollard, T. D. (1992) *Curr. Opin. Cell Biol.* **4,** 43–52.
3. De Lozanne, A. & Spudich, J. A. (1987) *Science* **236,** 1086–1091.
4. Knecht, D. A. & Loomis, W. F. (1987) *Science* **236,** 1081–1085.
5. Zang, J. H., Cavet, G., Sabry, J. H., Wagner, P., Moores, S. L. & Spudich, J. A. (1997) *Mol Biol. Cell* **8,** 2617–2629.
6. Neujahr, R., Heizer, C. & Gerisch, G. (1997) *J. Cell Sci.* **110,** 123–137.
7. Mueller, H. & Perry, S. V. (1962) *Biochem. J.* **85,** 431–439.
8. Toyoshima, Y. Y., Kron, S. J., McNally, E. M., Niebling, K. R., Toyoshima, C. & Spudich, J. A. (1987) *Nature (London)* **328,** 536–539.
9. Rayment, I., Rypniewski, W. R., Schmidt-Base, K., Smith, R., Tomchick, D. R., Benning, M. M., Winkelmann, D. A., Wesenberg, G. & Holden, H. M. (1993) *Science* **261,** 50–58.
10. Ruppel, K. M., Uyeda, T. Q. P. & Spudich, J. A. (1994) *J. Biol. Chem.* **269,** 18773–18780.
11. Sussman, M. (1987) *Methods Cell Biol.* **28,** 9–29.

12. Bradford, M. M. (1976) *Anal. Biochem.* **72,** 248–254.
13. Peltz, G., Spudich, J. A. & Parham, P. (1985) *J. Cell Biol.* **100,** 1016–1023.
14. Moores, S. L. & Spudich, J. A. (1998) *Mol. Cell* **1,** 1043–1050.
15. Sabry, J. H., Moores, S. L., Ryan, S., Zang, J.-H. & Spudich, J. A. (1997) *Mol. Biol. Cell* **8,** 2605–2615.
16. Egelhoff, T. T., Lee, R. J. & Spudich, J. A. (1993) *Cell* **75,** 363–371.
17. Clark, M. & Spudich, J. A. (1974) *J. Mol. Biol.* **86,** 209–222.
18. De Lozanne, A., Berlot, C. H., Leinwand, L. A. & Spudich, J. A. (1987) *J. Cell Biol.* **105,** 2999–3005.
19. Moens, P. B. (1976) *J. Cell Biol.* **68,** 113–122.
20. Moores, S. L., Sabry, J. H. & Spudich, J. A. (1996) *Proc. Natl. Acad. Sci. USA* **93,** 443–446.
21. Bray, D. & White, J. G. (1988) *Science* **239,** 883–888.
22. Rappaport, R. (1971) *Int. Rev. Cytol.* **105,** 245–281.
23. White, J. G. & Borisy, G. G. (1983) *J. Theor. Biol.* **101,** 289–316.
24. Yumura, S. & Uyeda, T. Q. (1997) *Mol Biol. Cell* **8,** 2089–2099.
25. Niswonger, M. L. & O'Halloran, T. J. (1997) *Proc. Natl. Acad. Sci. USA* **94,** 8575–8578.
26. Vallee, R. B., Shpetner, H. S. & Paschal, B. M. (1990) *Ann. N.Y. Acad. Sci.* **582,** 99–107.
27. Williams, B. C., Riedy, M. F., Williams, E. V., Gatti, M. & Goldberg, M. L. (1985) *J. Cell Biol.* **129,** 709–723.
28. Giansanti, M. G., Bonaccorsi, S., Williams, B., Williams, E. V., Santolamazza, C., Goldberg, M. & Gatti, M. (1998) *Genes Dev.* **12,** 396–410.
29. Adams, R. R., Tavares, A. A., Salzberg, A., Bellen, H. J. & Glover, D. M. (1998) *Genes Dev.* **12,** 1483–1494.
30. Rappaport, R. (1961) *J. Exp. Zool.* **148,** 81–89.
31. Rappaport, R. (1996) *Cytokinesis in Animal Cells* (Cambridge Univ. Press, Cambridge, U.K.).